

From Slots to Tubes: The Influence of Dimensionality on Fracture Dissolution Models

Piotr SZYMCZAK

Institute of Theoretical Physics, Faculty of Physics, University of Warsaw,
Warszawa, Poland; e-mail: Piotr.Szymczak@fuw.edu.pl

Abstract

We briefly review the models of fracture dissolution process, discussing the experimental and numerical evidence showing that this phenomenon is inherently two-dimensional and hence cannot be accurately described by one-dimensional models. The physical reason for this incompatibility is that a dissolution front in a single rock fracture is potentially unstable to small variations in local permeability, leading to spontaneous formation of dissolution channels in the rock. This leads to a dramatic increase of fissure opening rates, which must be taken into account not only in the estimation of karstification times but also in the assessment of ground subsidence, dam collapse or toxic seepage risks.

Key words: dissolution, karst formation, hydrology.

1. INTRODUCTION

About one fifth of the Earth's surface is formed from carbonate rocks, and the variety of karst landscapes, with disappearing streams, fissures and giant caves, has always been intriguing (Trudgill 2008). The notion that caves result from dissolution by water containing carbon dioxide was already present in the works of Lyell and Thirria in the 1830s (Lyell 1830, Thirria 1830, Shaw 2000), but it was not until 100 years later that these ideas were developed in detail. A quantitative mathematical model of the dissolution of a single limestone fracture was developed by Weyl (1958), taking into account chemical kinetics and solute transport.

His theory led to the paradoxical conclusion that water flowing through a limestone fracture becomes saturated with calcium ions over length scales of the order of tens of centimeters, so that limestone caves should not exist at all (White and Longyear 1962). A possible resolution of this paradox was proposed by White (1977), who noted that the existence of large cave systems may be explained by a sharp drop in the dissolution rate of calcium carbonate near saturation; this is frequently referred to as the “kinetic trigger” mechanism in the speleogenesis literature.

Several independent calculations (Dreybrodt 1990, 1996, Palmer 1991, Groves and Howard 1994) have shown that the kinetic trigger hypothesis allows for the development of deep conduits, but the model proposed by Weyl (1958) is inherently one-dimensional. The initial fissure is approximated by two parallel planes, and all the quantities determining the dissolution process (solute concentration, aperture, and fluid velocity) depend only on the distance from the fluid inlet. This same assumption was adopted by later workers (Dreybrodt 1990, 1996, Palmer 1991, Groves and Howard 1994) as well. Here we discuss the evidence suggesting that this assumption may not be valid: a planar dissolution front in an entirely uniform fracture is unstable to infinitesimal perturbations leading to spontaneous formation of wormhole-like channels in the rock. These channels have a very high flow rate and can carry an under-saturated solution deep into the fracture, thus dramatically decreasing fracture opening times. Additionally, the presence of this instability can explain the morphological transition that takes place during the dissolution of limestone fractures leading to the formation of karst caves: Even though formation of caves starts along the initial fissures with slot-like geometries, the mature cave is almost always a system of tube-like conduits.

2. ONE-DIMENSIONAL MODEL OF FRACTURE DISSOLUTION

In this paper, we will consider the dissolution of a single rock fracture, a system like that shown in Fig. 1. The fracture is characterized by its length L , width W , and the aperture field $h(x, y)$ (with the vertical axis, z , perpendicular to the rock surfaces). There is a reactive fluid flowing through the system along the x direction, driven by a pressure difference imposed between $x = 0$ and $x = L$.

In natural fractures the aperture is typically less than 1 mm, while the length and width are of the order of meters. This difference of scales is usually exploited in the construction of the models of the fracture dissolution process. The relevant physical fields, such as the reactant concentration profiles, are usually averaged over the aperture and the thin film (lubrication) approximation is used to calculate the flow.

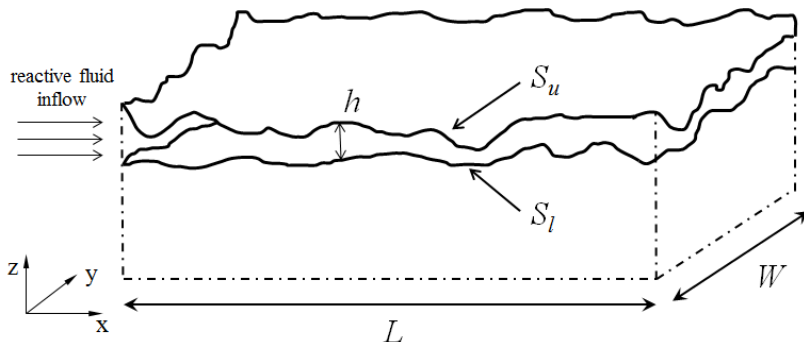


Fig. 1. A schematic view of a system: a fracture of length L and width W dissolved by a reactive fluid flowing along x direction. The aperture, $h(x, y)$, is the distance between the lower surface (S_l) and the upper surface (S_u).

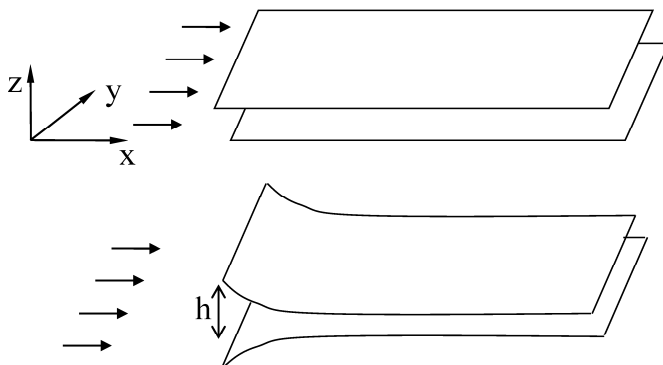


Fig. 2. Dissolution of a one-dimensional fracture; fluid flow is in the x direction and the fracture surfaces dissolve in the normal (z) direction. The fracture surfaces can be assumed to be located at $\pm h/2$.

Undoubtedly, the simplest models of the dissolving fractures are the so-called 1D models, in which it is assumed that all the relevant quantities such as the fracture aperture h or reactant concentration c depend on a single spatial variable only, namely the distance from the inlet. The underlying picture is then that of a fracture which opens uniformly along its width, as illustrated in Fig. 2.

These models, originally introduced by Weyl (1958), are still used in speleogenesis literature (Dreybrodt 1990, 1996, Groves and Howard 1994, Dijk and Berkowitz 1998). The basic elements of these models are the following. The flow in the fracture is calculated using a thin-film (Reynolds) approximation

$$q_0 = \frac{\Delta p}{R(t)} , \quad R(t) = 12\mu \int_0^L \frac{dx}{h(x,t)^3} , \quad (1)$$

where q_0 is the depth-integrated flux, $q_0 = \int_0^h v_x(z) dz$, Δp is the difference between the inlet and outlet pressures, and R is the integrated flow resistivity. The concentration of Ca^{2+} ions in the fracture, $c(x, t)$, is described by a convection-diffusion equation

$$q \frac{dc}{dx} - \frac{d}{dx} \left(hD \frac{dc}{dx} \right) = 2R(c) , \quad (2)$$

where D is the dispersion coefficient, and $R(c)$ is the reactive flux from the dissolving calcite. The factor of two in the dissolution rate comes from combining erosion at the upper and lower fracture surfaces. It is assumed that the inlet stream is pure water, $c(0, t) = 0$. Finally, the aperture evolution is determined from the local reactive flux

$$c_{\text{sol}} \frac{dh}{dt} = 2R(c) , \quad (3)$$

where c_{sol} is the molar concentration of the solid phase. For the dissolution of the limestone fractures by natural groundwater the controlling factor is the undersaturation of the calcium ions, and the reactive flux takes the form

$$R(c) = r(c_{\text{sat}} - c) . \quad (4)$$

Let us look at the predictions of this model in the simplest case when the flow through the fracture is assumed to be constant in time and the axial dispersion is neglected. Equations (2)-(4) can then be solved to yield the concentration profile

$$c_{ld}(x) = c_{\text{sat}} \left(1 - e^{-2rx/q_0} \right) , \quad (5)$$

and

$$h_{ld}(x) = h_0 + 2r\gamma te^{-2rx/q_0} , \quad (6)$$

with $\gamma = c_{\text{sat}}/c_{\text{sol}}$. The important observation is that these profiles are exponential, $c, h \sim \exp(-x/l_p)$ with the penetration length

$$l_p = \frac{q_0}{2r} \quad (7)$$

Let us now try to estimate the characteristic value of l_p for the real systems. The typical values of the parameters characterizing the dissolution of limestone fractures are: $r = 2.5 \times 10^{-5} \text{ cm s}^{-1}$, $c_{\text{sat}} = 2 \times 10^{-6} \text{ M cm}^{-3}$, and $c_{\text{sol}} = 0.027 \text{ M cm}^{-3}$ (Dreybrodt 1996). Initial fracture apertures are between

0.005 and 0.1 cm (Motyka and Wilk 1984, Dreybrodt 1996, Paillet *et al.* 1987), and hydraulic gradients are of the order of 10^{-3} to 10^{-1} (Palmer 1991, Dijk and Berkowitz 1998). This gives a range of characteristic flow velocities in undissolved fractures from 10^{-4} to 1 cm/s. For these parameter values, the penetration lengths are of the order of centimetres: *e.g.*, for $h_0 = 0.02$ mm and the hydraulic gradient of 0.01, we get $q_0 = 10^{-3} \text{ cm}^2 \text{s}^{-1}$ and $l_p \approx 20$ cm. This is exceedingly small when compared to the lengths of the fractures (100 m - 10 km). Thus the groundwater quickly saturates with the calcium ions and long karst conduits cannot be formed, at least within the framework of the present model. This was noted by White and Longyear (1962), but, interestingly, a similar argument was also raised by Armande Flamache in 1895 (Flamache 1895, Shaw 2000), and was a basis for his dismissal of a dissolution mechanism for cave formation.

One resolution of this paradox has been suggested by White (1977), who, based on the experimental data on calcite dissolution (Plummer and Wigley 1976), noted that the existence of large cave systems may be explained by the sharp drop in the dissolution rate of CaCO_3 near saturation; this is frequently referred to as the “kinetic trigger” mechanism in the speleogenesis literature. The “kinetic trigger” can be modelled as a switch from linear to higher order kinetics at a threshold concentration c_{th} :

$$R(c) = \begin{cases} r(c_{\text{sat}} - c), & c < c_{\text{th}} \\ r_n(c_{\text{sat}} - c)^n, & c > c_{\text{th}} \end{cases} \quad (8)$$

A nonlinear reaction law ($n > 1$) results then in a power-law concentration profile

$$c_s - c \sim x^{\frac{1}{1-n}} \quad (9)$$

instead of an exponential one (5). This increases the penetration depths and leads to fracture opening over the geologically reasonable timescales, at least in the case of the fractures of relatively large initial aperture (Dreybrodt 1990, 1996).

3. TWO-DIMENSIONAL MODELS

The one-dimensional models of fracture dissolution remain attractive due to their simplicity and analytical tractability. However, a basic requirement for such models to be applicable to real fractures is that the dissolution processes are indeed uniform along the direction transverse to the flow. Yet, a number of results, both experimental and computational, suggest that highly localized two-dimensional dissolution patterns can be formed during fracture dissolution (*cf.* Fig. 3). On the experimental side, in recent years there were several studies (Durham *et al.* 2001, Detwiler *et al.* 2003, Gouze *et al.* 2003) which demonstrated the creation of distinct dissolution channels,

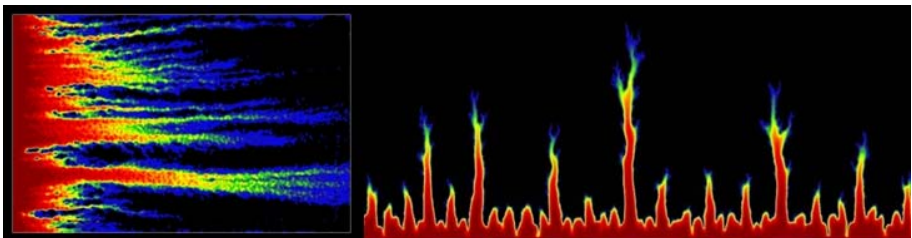


Fig. 3. Examples of localized patterns in fracture dissolution: the experimental results of Detwiler *et al.* (2003) and the results of numerical simulations of fracture dissolution by Szymczak and Ladd (2006). The red shading indicates the deepest erosion while dark gray/blue indicates the least erosion; the intermediate colors are yellow (higher) and green (lower). Colour version of this figure is available in electronic edition only.

chemically eroded in the fracture walls by the reactant (*cf.* the left panel of Fig. 3). This was confirmed by the numerical studies, most notably work by Rajaram and collaborators (Hanna and Rajaram 1998, Cheung and Rajaram 2002, Detwiler and Rajaram 2007, Rajaram *et al.* 2009) as well as Szymczak and Ladd (2004, 2006, 2009). An example dissolution pattern from the latter study is shown in the right panel of Fig. 3.

Undoubtedly, the most striking examples of nonuniform dissolution can be found in limestone caves itself. Even though formation of caves starts along the fractures and bedding planes, which have *quasi* 2D, slot-like geometries, the mature cave is almost always a system of pipe-like conduits, such as the one depicted in Fig. 4. This suggests that the fracture dissolution is inherently a 2D process, and 1D model might not be applicable here.

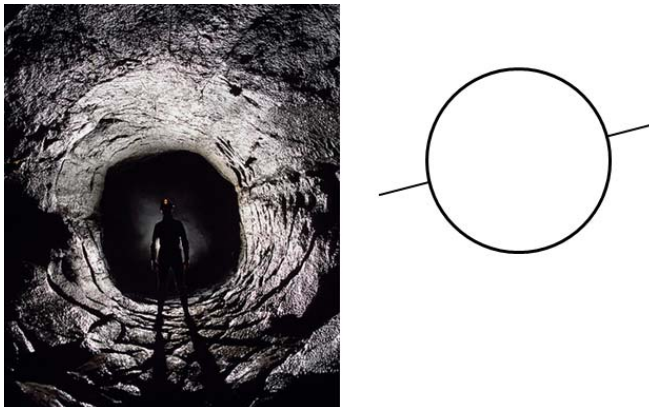


Fig. 4. The conduit in a phreatic cave in Dan Yr Ogof, Swansea Valley, South Wales (photo courtesy of Brendan Marrs, Dudley Caving Club) (left); and a schematic cross section of the conduit, showing the initial fissure (right).

A more formal proof of this fact was given by Szymczak and Ladd (2011a), who have shown that the 1D solutions given by Eqs. (5) and (6) are unstable with respect to infinitesimal perturbations in the direction transverse to the flow. In order to demonstrate this, one should formulate first a 2D model of a dissolving fracture, which treats the aperture as a function of both x and y . One of such models is a “depth-averaged” model proposed by Hanna and Rajaram (1998) (see also Detwiler and Rajaram 2007, Rajaram *et al.* 2009, Szymczak and Ladd 2012), in which the fluid velocity and reactant concentration are still averaged over the fracture aperture (z direction in Fig. 1), but can vary in the lateral (y) direction. The depth-integrated fluid flux, $\mathbf{q}(x,y)$, is again calculated based on the thin-film approximation:

$$\mathbf{q}(x,y) = -\frac{h(x,y)^3}{12\eta} \nabla p(x,y) , \quad \nabla \cdot \mathbf{q}(x,y) = 0 , \quad (10)$$

whereas the transport equation for the depth-averaged concentration of dissolved solids $c(x,y)$ is given by

$$\nabla \cdot (\mathbf{q}c) - \nabla \cdot (hD\nabla c) = 2r(c_s - c) . \quad (11)$$

This is supplemented by the erosion equation,

$$c_{\text{sol}} \frac{dh}{dt} = 2R(c) \quad (12)$$

identical to that in 1D model. A detailed derivation of the 2D equations, together with the discussion of their limits of applicability is given in Appendix A of Szymczak and Ladd (2012). Next, to investigate the stability of 1D solutions, we consider infinitesimal perturbations to the base profiles (5) and (6)

$$c(x,y,t) = c_{1d}(x) + \delta c(x) \cos ky e^{\sigma t} , \quad (13)$$

$$h(x,y,t) = h_{1d}(x,t) + \delta h(x) \cos ky e^{\sigma t} , \quad (14)$$

and similarly for the pressure field:

$$p(x,y,t) = p_{1d}(x) + \delta p(x) \cos ky e^{\sigma t} , \quad (15)$$

where $p_{1d}(x)$ is the linear pressure profile corresponding to the fluid flux q_0 . In the convective limit (*i.e.*, when the dispersion term in Eq. (11) is neglected) this leads to a dispersion relation for the growth rate σ as a function of the wavenumber of the perturbation k , as shown in Fig. 5.

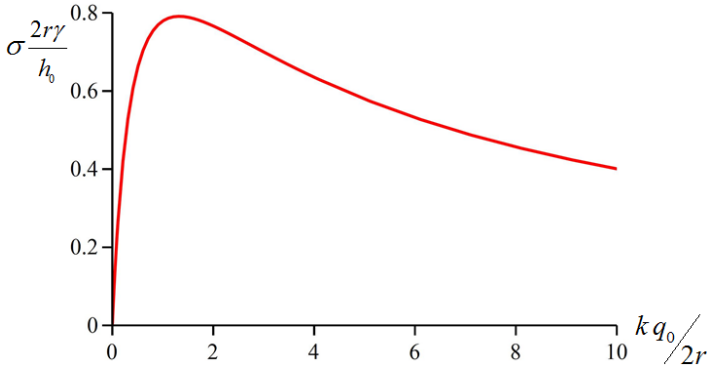


Fig. 5. The dispersion relation $\sigma(k)$, which gives the growth rates of the instability as a function of the wavenumber of the perturbation along y direction (Szymczak and Ladd 2011a). The parameters h_0 and q_0 correspond to the mean aperture and depth-averaged fluid flux in the initial, uniform fracture.

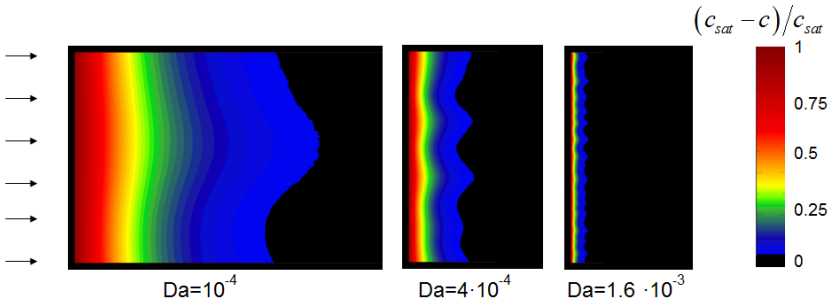


Fig. 6. Concentration profiles of a dissolving fracture. Contour plots of the undersaturation, $(c_{\text{sat}} - c)/c_{\text{sat}}$, are plotted for different Damköhler numbers, $\text{Da} = 2rh_0/q_0$. Colour version of this figure is available in electronic edition only.

As observed in Fig. 5, in the whole range of wavenumbers the growth is unstable, $\sigma(k) > 0$, thus, at least in the convective limit, the fracture dissolution is inherently two dimensional. Another striking feature of $\sigma(k)$ relation is that there is a maximal growth rate, $\sigma_{\max} = 0.79 h_0/2\gamma$, at a wavenumber $k_{\max} = 1.32 2r/q_0$; this mode should then be most strongly enhanced during the initial growth. Thus the maximally unstable wavelength is inversely proportional to the Damköhler number, $\text{Da} = 2rh_0/q_0$, which relates the surface reaction rate to the mean fluid velocity. This proportionality is fully confirmed by the results of the numerical simulations of the dissolution of smooth fractures (Szymczak and Ladd 2011a), as shown in Fig. 6.

The above results were obtained for the simplest case of the reaction-limited, convective-dominated dissolution in a fracture of infinite extent. A more involved analysis, where some or all of these assumptions are re-

laxed, is presented in Szymczak and Ladd (2012). The general conclusions remain essentially unchanged: even with diffusive effects included, the dissolution remains unstable over all wavelengths; the most pronounced effect of the diffusion being a shift of the peak growth rate towards longer wavelength.

Fig. 7 shows the dispersion curves obtained with different amount of diffusion, as measured by the dimensionless parameter $H = 2Drh_0/q_0^2$. The importance of this parameter in assessment of the relative contribution of diffusive and convective transport in reactive flow problems is discussed, e.g., in Phillips (1990), Steefel and Lasaga (1990), and Szymczak and Ladd (2012).

The instability described above is in many ways similar to the so-called reactive-infiltration instability in a dissolving porous medium (Chadam *et al.* 1986, Ortoleva *et al.* 1987, Sherwood 1987, Hinch and Bhatt 1990), however there are also important differences between the two, most notably in the 1D base profiles the stability of which one is investigating (Fig. 8): whereas in the fracture it is a steadily opening exponential aperture profile (6), in porous media, since the maximum possible porosity is bounded from above, a steadily propagating, invariant porosity profile is formed

$$\varphi(x) = \varphi_0 + (\varphi_{\max} - \varphi_0)e^{-(x-Vt)/l_p}, \quad (16)$$

moving with velocity V towards the outlet. Here, φ_0 is the initial value of porosity in undissolved medium whereas φ_{\max} is the final porosity formed after

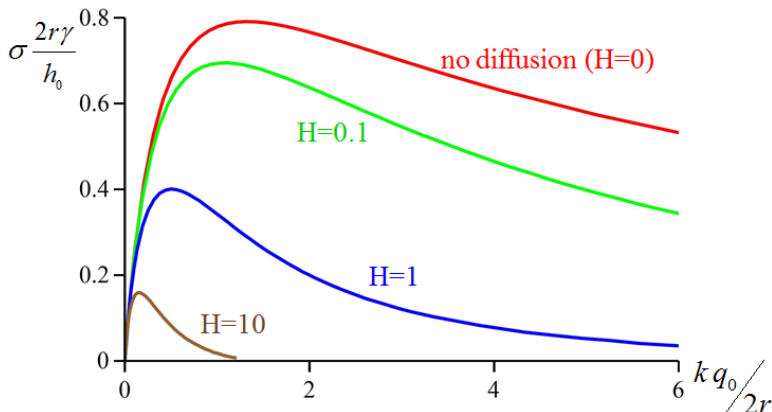


Fig. 7. The dispersion relation $\sigma(k)$, obtained with different amounts of diffusion as measured by the dimensionless parameter $H = 2Drh_0/q_0^2$ (Szymczak and Ladd 2012). Colour version of this figure is available in electronic edition only.

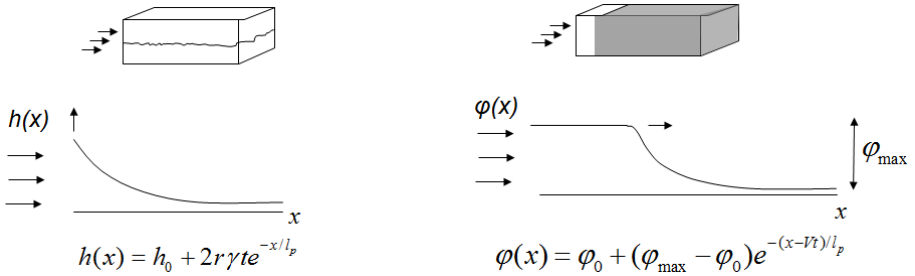


Fig. 8. Sketch illustrating the differences between the 1D aperture profile in a dissolving fracture (left) and the steadily advancing porosity profile in a dissolving porous rock (right).

all the soluble materials have dissolved. Interestingly, both profiles (6) and (16) are unstable, but the dispersion relations associated with these instabilities are in general different (Szymczak and Ladd 2011b).

In the later stages of the dissolution the undulations of the front are transformed into well-defined finger-like channels which rapidly advance, causing dissolutional opening of the fracture at much earlier times than in the homogeneous (one-dimensional) case. As dissolution proceeds, the fingers interact, competing for the available flow, and eventually the growth of the shorter ones cease (*cf.* Fig. 9). The mechanism of the competition is further elucidated in Fig. 10 – as observed, there are many more fingers visible in the aperture map (center) than in either concentration (left) or flow map (right). In fact the longer channels suck up the flow from the shorter ones by a mechanism described in Szymczak and Ladd (2006). In short, the pressure gradient in the long channel is steeper than in the short channel, because the flow rate is higher. In the upstream part of the fracture the short channel is therefore at a higher pressure than the long one, so the flow in the surrounding matrix is directed towards the long channel. Downstream the situation is reversed with the region around the tip of the long channel at a higher pressure than the surrounding medium and so flow is directed away from the channel, which is indeed observed near the tips of the channels in Fig. 10.

The shorter channels, devoid of the flow, quickly become saturated and stop growing, thus losing the competition. On the other hand, the longer channels again compete for the flow between themselves which leads to the emergence of a hierarchical structure, with many short channels, and only a few long ones (center panel in Fig. 10). Hence the characteristic distance between the active channels, \$d\$, steadily increases. The characteristic flow within the active channels, \$q^{\text{chann}}\$, increases as well, approximately in the proportion to \$d/w\$:

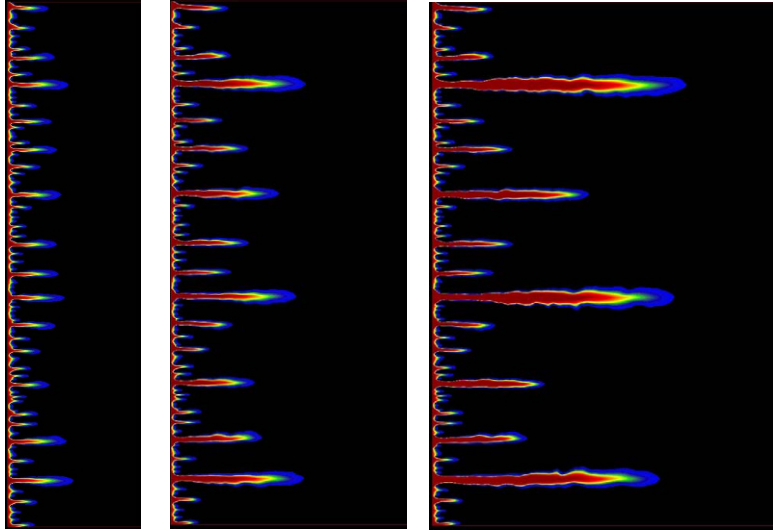


Fig. 9. Evolution of the aperture field in time; the competition between the channels gives rise to the emergence of a hierarchical pattern with many short channels and a few long ones. Colour version of this figure is available in electronic edition only.

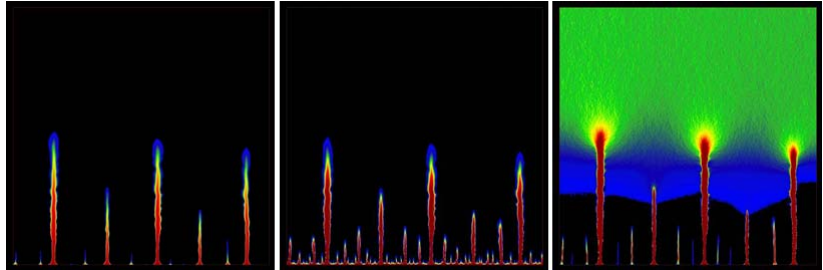


Fig. 10. Concentration (left), aperture (center), and flow profiles (right) in a dissolving fracture. Red shading indicates the regions of highest undersaturation/aperture/flow magnitude, followed by green, blue, and black. Colour version of this figure is available in electronic edition only.

$$q^{\text{chann}} = q_0 d/w , \quad (17)$$

where w is the characteristic width of the channel (*cf.* Fig. 11). Eventually, d reaches the scale of the width of the fracture, W , when there is only one active channel left in the system. At that moment the penetration length in the channel approaches

$$l_p^{\text{chann}} = \frac{q_0 W}{2rw} , \quad (18)$$

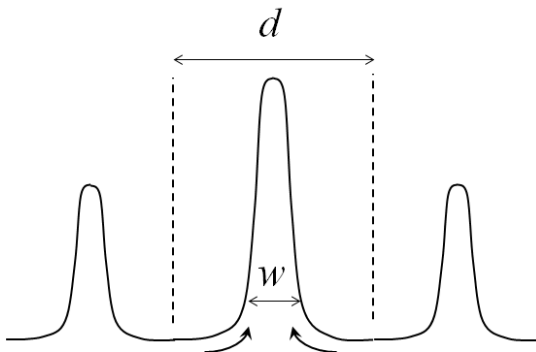


Fig. 11. Flow focusing in the dissolution channels: the channel of width w attracts the flow from the region of a linear extent d (equal to the characteristic distance between the channels).

which is usually several orders of magnitude larger than the initial penetration length given by Eq. (7). Thus the flow focusing in the channels provides an alternative mechanism for the increase of penetration length and hence for the possibility of karst conduit formation, even in the absence of a kinetic trigger.

Finally, following Szymczak and Ladd (2011a) let us compare the fracture opening times calculated using different models for a $20\text{ m} \times 10\text{ m} \times 0.2\text{ mm}$ limestone fracture with a very small initial roughness ($st(h)/\langle h \rangle = 10^{-6}$ where $st(h)$ is the standard deviation of the initial aperture field, whereas $\langle h \rangle$ is its average value). This time the constant pressure drop boundary conditions are imposed, thus the flow is allowed to vary in time. Fig. 12 shows the comparison of time-dependent flow rates from 1D and 2D simulations, as reported in Szymczak and Ladd (2011a).

A characteristic feature of these graphs is a rapid, near vertical increase in the flow at the “breakthrough time”, *i.e.*, the time at which the dissolution reaches the outlet of the fracture. Such a rapid permeability increase near breakthrough is a feature characteristic for the dissolution problems (Hoefner and Fogler 1988, Hanna and Rajaram 1998, Cheung and Rajaram 2002, Chaudhuri *et al.* 2008). As expected, two-dimensional simulations show a significant reduction in the breakthrough time in comparison with 1D models. The most important observation, however, is that in 2D simulations the nonlinear (“kinetic trigger”) kinetics has almost no effect on the breakthrough time. This is because due to the large flows in the dissolution channels the undersaturation there is high, above the threshold for non-linear kinetics.

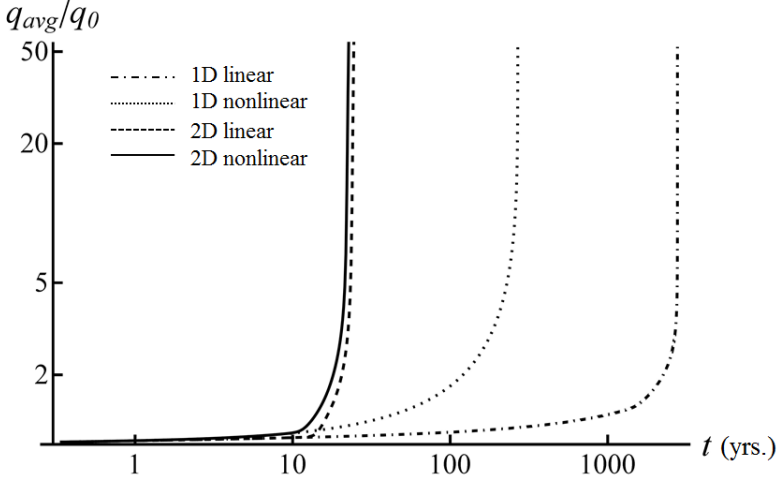


Fig. 12. Dissolution of a smooth fracture $20\text{ m} \times 10\text{ m} \times 0.2\text{ mm}$; with $\text{Da} = 5 \times 10^{-4}$ and $q_0/D = 100$. The fluid flux $q(t)$ obtained from the one-dimensional simulations is compared with the average flux $q_{\text{avg}}(t) = W^{-1} \int_0^W q_x(x, y, t) dy$ from the two-dimensional simulations. The fluxes are scaled by the initial flux in the fracture q_0 .

Interestingly, channeling has been also observed in the karst formation in the hydrothermal settings (Andre and Rajaram 2005, Chaudhuri *et al.* 2008, 2009, Rajaram *et al.* 2009), however the physical mechanism behind its formation is somewhat different than that described above. In such systems, the limestone dissolution rate couples not only to the flow but also to the geothermal temperature gradient, since the solubility of calcite increases with decreasing temperature. This coupling has been shown to lead to the formation of extended conduit system (Andre and Rajaram 2005, Chaudhuri *et al.* 2008, Rajaram *et al.* 2009). Additionally, as the initial fracture aperture is increased, the buoyant convective flow arises which contributes to the development of the channeling patterns (Steefel and Lasaga 1994, Chaudhuri *et al.* 2009, Rajaram *et al.* 2009, Oltéan *et al.* 2013).

4. SUMMARY

In this paper we have reviewed the one- and two-dimensional models of fracture dissolution. As discussed, the experimental and numerical evidence seems to suggest that 1D models, although attractively simple, cannot be used to predict the evolution of dissolving fractures due to the inherent instability of a fracture dissolution process, which leads to the focusing of the flow in the dissolution channels. Interestingly, the order of the reaction ki-

netics on the dissolution dynamics turns out to be of much less importance for the estimate of the breakthrough time than suggested by one-dimensional models. A correct estimate of fracture opening times is crucial not only for an understanding of cave formation, but other geotechnical problems as well, such as the potential leakage of sequestered carbon dioxide, the safety of dam sites in soluble rocks, the risk of catastrophic ground subsidence due to the solutional widening of fractures, and the danger of water seepage into toxic waste repositories.

Acknowledgments. This work was supported by the National Science Centre (Poland) under research Grant No. 2012/07/E/ST3/01734. We thank Brendan Marris (Dudley Caving Club) for the permission to reproduce the image in Fig. 4. We thank Russell Detwiler (University of California, Irvine, USA) for providing us with the fracture profiles used to plot Fig. 3.

References

- Andre, B.J., and H. Rajaram (2005), Dissolution of limestone fractures by cooling waters: Early development of hypogene karst systems, *Water Resour. Res.* **41**, 1, 1-16, W01015, DOI: 10.1029/2004WR003331.
- Chadam, J., D. Hoff, E. Merino, P. Ortoleva, and A. Sen (1986), Reactive infiltration instabilities, *IMA J. Appl. Math.* **36**, 3, 207-221, DOI: 10.1093/imamat/36.3.207.
- Chaudhuri, A., H. Rajaram, and H. Viswanathan (2008), Alteration of fractures by precipitation and dissolution in gradient reaction environments: Computational results and stochastic analysis, *Water Resour. Res.* **44**, 10, W10410, DOI: 10.1029/2008WR006982.
- Chaudhuri, A., H. Rajaram, H. Viswanathan, G. Zyvoloski, and P. Stauffer (2009), Buoyant convection resulting from dissolution and permeability growth in vertical limestone fractures, *Geophys. Res. Lett.* **36**, 3, L03401, DOI: 10.1029/2008GL036533.
- Cheung, W., and H. Rajaram (2002), Dissolution finger growth in variable aperture fractures: Role of the tip-region flow field, *Geophys. Res. Lett.* **29**, 22, 32-1-32-4, DOI: 10.1029/2002GL015196.
- Detwiler, R.L., and H. Rajaram (2007), Predicting dissolution patterns in variable aperture fractures: Evaluation of an enhanced depth-averaged computational model, *Water Resour. Res.* **43**, 4, W04403, DOI: 10.1029/2006WR005147.
- Detwiler, R.L., R.J. Glass, and W.L. Bourcier (2003), Experimental observations of fracture dissolution: The role of Peclet number on evolving aperture

- variability, *Geophys. Res. Lett.* **30**, 12, 1648, DOI: 10.1029/2003GL017396.
- Dijk, P., and B. Berkowitz (1998), Precipitation and dissolution of reactive solutes in fractures, *Water Resour. Res.* **34**, 3, 457-470, DOI: 10.1029/97WR03238.
- Dreybrodt, W. (1990), The role of dissolution kinetics in the development of karst aquifers in limestone: a model simulation of karst evolution, *J. Geol.* **98**, 5, 639-655, DOI: 10.1086/629431.
- Dreybrodt, W. (1996), Principles of early development of karst conduits under natural and man-made conditions revealed by mathematical analysis of numerical models, *Water Resour. Res.* **32**, 9, 2923-2935, DOI: 10.1029/96WR01332.
- Durham, W.B., W.L. Bourcier, and E.A. Burton (2001), Direct observation of reactive flow in a single fracture, *Water Resour. Res.* **37**, 1, 1-12, DOI: 10.1029/2000WR900228.
- Flamache, A. (1895), Sur la formation des grottes et des vallées souterraines, *Bull. Soc. Belge Géol. Paléontol. Hydrol.* **9**, 355-367 (in French).
- Gouze, P., C. Noiriel, C. Bruderer, D. Loggia, and R. Leprevost (2003), X-ray tomography characterization of fracture surfaces during dissolution, *Geophys. Res. Lett.* **30**, 5, 1267, DOI: 10.1029/2002GL016755.
- Groves, C.G., and A.D. Howard (1994), Minimum hydrochemical conditions allowing limestone cave development, *Water Resour. Res.* **30**, 3, 607-615, DOI: 10.1029/93WR02945.
- Hanna, R.B., and H. Rajaram (1998), Influence of aperture variability on dissolutional growth of fissures in karst formations, *Water Resour. Res.* **34**, 11, 2843-2853, DOI: 10.1029/98WR01528.
- Hinch, E.J., and B.S. Bhatt (1990), Stability of an acid front moving through porous rock, *J. Fluid Mech.* **212**, 279-288, DOI: 10.1017/S0022112090001963.
- Hoefner, M.L., and H.S. Fogler (1988), Pore evolution and channel formation during flow and reaction in porous media, *AICHE J.* **34**, 1, 45-54, DOI: 10.1002/aic.690340107.
- Lyell, C. (1830), *Principles of Geology*, John Murray, London.
- Motyka, J., and Z. Wilk (1984), Hydraulic structure of karst-fissured Triassic rocks in the vicinity of Olkus (Poland), *Kras i Speleologia* **14**, 5, 11-24.
- Oltéan, C., F. Golfier, and M.A. Buès (2013), Numerical and experimental investigation of buoyancy-driven dissolution in vertical fracture, *J. Geophys. Res.* **118**, 5, 2038-2048, DOI: 10.1002/jgrb.50188.
- Ortoleva, P., J. Chadam, E. Merino, and A. Sen (1987), Geochemical self-organization II: The reactive-infiltration instability, *Am. J. Sci.* **287**, 1008-1040, DOI: 10.2475/ajs.287.10.1008.
- Paillet, F.L., A.E. Hess, C.H. Cheng, and E. Hardin (1987), Characterization of fracture permeability with high-resolution vertical flow measurements

- during borehole pumping, *Groundwater* **25**, 1, 28-40, DOI: 10.1111/j.1745-6584.1987.tb02113.x.
- Palmer, A.N. (1991), Origin and morphology of limestone caves, *Geol. Soc. Am. Bull.* **103**, 1, 1-21, DOI: 10.1130/0016-7606(1991)103<0001:OAMOLC>2.3.CO;2.
- Phillips, O.M. (1990), Flow-controlled reactions in rock fabrics, *J. Fluid Mech.* **212**, 263-278, DOI: 10.1017/S0022112090001951.
- Plummer, L.N., and T.M.L. Wigley (1976), The dissolution of calcite in CO₂-saturated solutions at 25°C and 1 atmosphere total pressure, *Geochim. Cosmochim. Ac.* **40**, 2, 191-202, DOI: 10.1016/0016-7037(76)90176-9.
- Rajaram, H., W. Cheung, and A. Chaudhuri (2009), Natural analogs for improved understanding of coupled processes in engineered Earth systems: examples from karst system evolution, *Curr. Sci. India.* **97**, 8, 1162-1176.
- Shaw, T.R. (2000), Views on cave formation before 1900. In: A.B. Klimchouk, D.C. Ford, A.N. Palmer, and W. Dreybrodt (eds.), *Speleogenesis: Evolution of Karst Aquifers*, National Speleological Society, Huntsville, 21-29.
- Sherwood, J.D. (1987), Stability of a plane reaction front in a porous medium, *Chemical Eng. Sci.* **42**, 7, 1823-1829, DOI: 10.1016/0009-2509(87)80187-2.
- Steefel, C.I., and A.C. Lasaga (1990), Evolution of dissolution patterns: permeability change due to coupled flow and reaction. In: D. Melchior, and R.L. Bassett (eds.), *Symp. American Chemical Society "Chemical Modeling in Aqueous Systems II"*, 25 September 1988, Los Angeles, USA, 212-225.
- Steefel, C.I., and A.C. Lasaga (1994), A coupled model for transport of multiple chemical species and kinetic precipitation/dissolution reactions with application to reactive flow in single phase hydrothermal systems, *Am. J. Sci.* **294**, 5, 529-592, DOI: 10.2475/ajs.294.5.529.
- Szymczak, P., and A.J.C. Ladd (2004), Microscopic simulations of fracture dissolution, *Geophys. Res. Lett.* **31**, 23, L23606, DOI: 10.1029/2004GL021297.
- Szymczak, P., and A.J.C. Ladd (2006), A network model of channel competition in fracture dissolution, *Geophys. Res. Lett.* **33**, 5, L05401, DOI: 10.1029/2005GL025334.
- Szymczak, P., and A.J.C. Ladd (2009), Wormhole formation in dissolving fractures, *J. Geophys. Res.* **114**, B6, B06203, DOI: 10.1029/2008JB006122.
- Szymczak, P., and A.J.C. Ladd (2011a), The initial stages of cave formation: Beyond the one-dimensional paradigm, *Earth Planet. Sci. Lett.* **301**, 3-4, 424-432, DOI: 10.1016/j.epsl.2010.10.026.
- Szymczak, P., and A.J.C. Ladd (2011b), Instabilities in the dissolution of a porous matrix, *Geophys. Res. Lett.* **38**, 7, L07403, DOI: 10.1029/2011GL046720.
- Szymczak, P., and A.J.C. Ladd (2012), Reactive-infiltration instabilities in rocks. Fracture dissolution, *J. Fluid Mech.* **702**, 239-264, DOI: 10.1017/jfm.2012.174.

- Thirria, M.E. (1830), Notice sur le terrain jurassique du département de la Haute-Saône et sur quelques grottes. In: *Mémoires de la Société d'histoire naturelle de Strasbourg*, F.G. Levrault, Paris (in French).
- Trudgill, S.T. (2008), Limestone landforms 1890-1965. In: T.P. Burt, R.J. Chorley, D. Brunsden, N.J. Cox, and A.S. Goudie (eds.), *The History of the Study of Landforms or the Development of Geomorphology*, Geol. Soc., London, 107-125.
- Weyl, P.K. (1958), The solution kinetics of calcite, *J. Geol.* **66**, 2, 163-176, DOI: 10.1086/626492.
- White, W.B. (1977), Role of solution kinetics in the development of karst aquifers. Karst hydrogeology, *Mem. Int. Assoc. Hydrogeol.* **12**, 503-517.
- White, W.B., and J. Longyear (1962), Some limitations on speleogenetic speculation imposed by the hydraulics of groundwater flow in limestone, *Nittany Grotto Newslett.* **10**, 155-167.